ISSN 1062-8738, Bulletin of the Russian Academy of Sciences: Physics, 2010, Vol. 74, No. 6, pp. 833–841. © Allerton Press, Inc., 2010.
Original Russian Text © V.V. Varlamov, B.S. Ishkhanov, V.N. Orlin, V.A. Chetvertkova, 2010, published in Izvestiya Rossiiskoi Akademii Nauk. Seriya Fizicheskaya, 2010, Vol. 74, No. 6, pp. 875–883.

Evaluated Cross Sections of the σ(γ, n*X*) and σ(γ, 2n*X*) Reactions on $^{112, 114, 116, 117, 118, 119, 120, 122, 124}$Sn Isotopes

V. V. Varlamov[a], B. S. Ishkhanov[a,b], V. N. Orlin[a], and V. A. Chetvertkova[a]

[a] *Skobeltsyn Institute of Nuclear Physics, Moscow State University, Moscow, 119991 Russia*

[b] *Physics Faculty, Moscow State University, Moscow, 119991 Russia*

e-mail: Varlamov@depni.sinp.msu.ru

Abstract—A combined analysis of experimental data on total and partial photoneutron reaction cross sections, obtained using bremsstrahlung γ-radiation and quasi-monoenergetic annihilation photon beams, was performed for nine Sn isotopes. The partial reactions $\sigma^{eval}(\gamma, nX)$ and $\sigma^{eval}(\gamma, 2nX)$ cross sections were evaluated using an approach free of the shortcomings of experimental neutron multiplicity sorting methods. This approach involves calculations within the photonuclear reaction model, based on Fermi gas densities and considering the effects of nucleus deformation, the isospin splitting of its giant dipole resonance (GDR), and experimental data on the total photoneutron cross sections $\sigma^{exp}(\gamma, xn) = \sigma^{exp}(\gamma, nX) + 2\sigma^{exp}(\gamma, 2nX) = \sigma^{exp}(\gamma, n) + \sigma^{exp}(\gamma, np) + ... + 2\sigma^{exp}(\gamma, 2n) + 2\sigma^{exp}(\gamma, 2np) + ...$ The evaluated $\sigma^{eval}(\gamma, nX)$ and $\sigma^{eval}(\gamma, 2nX)$ reactions cross sections were obtained using the introduced transition multiplicity functions $F^{theor} = \sigma^{theor}(\gamma, 2nX)/\sigma^{theor}(\gamma, xn) = \sigma^{theor}(\gamma, 2nX)/[\sigma^{theor}(\gamma, nX) + 2\sigma^{theor}(\gamma, 2nX) + ...]$; and $\sigma^{eval}(\gamma, 2nX) = F^{theor}\sigma^{exp}(\gamma, xn) = \sigma^{eval}(\gamma, nX) = (1 - 2F^{theor})\sigma^{exp}(\gamma, xn)$. The evaluated partial reaction cross sections were used to assess the total photoneutron reaction cross sections $\sigma^{eval}(\gamma, sn) = \sigma^{eval}(\gamma, nX) + \sigma^{eval}(\gamma, 2nX) + ...$ as functions of the mass number *A*. The GDR features of $^{112, 114, 116, 117, 118, 119, 120, 122, 124}$Sn isotopes were studied and are discussed here.

DOI: 10.3103/S1062873810060225

INTRODUCTION

As a result of γ-quantum absorption by the nucleus in the energy region of the giant dipole resonance (GDR), the excited nucleus emits individual nucleons or combinations of them. One nucleon is emitted with the highest probability, while two or more nucleons are emitted with a lower probability. This, in combination with the relations of the energy thresholds of corresponding reactions, defines the σ(γ, *abs*) total photoabsorption cross section and the main GDR decay channels,

$$\sigma(\gamma, abs) = \sigma(\gamma, n) + \sigma(\gamma, np) + \sigma(\gamma, n2p) + \sigma(\gamma, 2n) + ... + \sigma(\gamma, 2np) + \sigma(\gamma, 2n2p) + ... + \sigma(\gamma, 3n) + \sigma(\gamma, 3np) + \sigma(\gamma, 3n2p) + ... + \sigma(\gamma, f). \quad (1)$$

The relation between the cross sections of the photoneutron reactions that produce different numbers of neutrons is an important characteristic of the photodisintegration process, which depends on nucleus excitation and decay mechanisms. Experimental studies of the photonuclear reactions that produce different numbers of neutrons is, however, a problem whose complexity is due mainly to the energy thresholds of different partial reactions [1] being close to one another (Table 1).

When neutrons are detected in the energy region above (γ, 2n) reaction energy threshold B_{2n}, it is necessary to identify the reaction, (γ, n),(γ, 2n), (γ, 3n), ..., in which it was produced. Otherwise, direct experimental photoneutron detection can yield only the total photoneutron reaction cross section

$$\sigma(\gamma, xn) \approx \sigma(\gamma, n) + 2\sigma(\gamma, 2n) + 3\sigma(\gamma, 3n) + 4\sigma(\gamma, 4n) + ..., \quad (2)$$

which includes the partial cross sections σ(γ, 2n), σ(γ, 3n), σ(γ, 4n), ... with corresponding multiplicity coefficients, i.e., 2, 3, 4, ...

As is seen in Table 1, channels in which neutron emission is accompanied by proton emission should be considered in addition to pure neutron channels in studies of Sn isotope photodisintegration. For $^{112, 114, 116}$Sn isotopes, e.g., $B_p < B_n$; for some isotopes, $B_{np} \approx B_{2n}$. Therefore, instead of (2), it is more correct to use the relation

$$\sigma(\gamma, xn) \approx \sigma(\gamma, nX) + 2\sigma(\gamma, 2nX) + 3\sigma(\gamma, 3nX) + ..., \quad (3)$$

in which *X* denotes the sum of all processes in which emission of one, two, three, ... neutrons is accompanied by other particles (or their combinations). In the energy region under consideration ($E < 25$ MeV), the σ(γ, 3n*X*) reaction cross section and (even more so) the cross sections of reactions that produce a larger number of neutrons, are small. Moreover, there are

Table 1. Abundances of the studied stable Sn isotopes in a natural mixture and the thresholds of the main photonuclear reactions on Sn isotopes

Isotope	Abundance, %	Reaction thresholds, MeV								
		B_n	B_p	B_{2n}	B_{2p}	B_{np}	B_{3n}	B_{3p}	B_{2np}	B_{4n}
^{112}Sn	0.97	10.8	7.6	19.0	12.9	17.6	30.2	21.8	25.6	38.9
^{114}Sn	0.65	10.3	8.5	18.0	14.6	17.9	28.8	24.2	25.6	37.0
^{116}Sn	14.53	9.6	9.3	17.1	16.1	18.3	27.4	26.4	25.6	35.2
^{117}Sn	7.68	6.9	9.4	16.5	16.9	16.2	24.1	27.3	25.3	34.4
^{118}Sn	24.23	9.3	10.0	16.3	17.5	18.8	25.8	28.5	25.6	33.4
^{119}Sn	8.59	6.5	10.1	15.8	18.2	16.5	22.8	29.4	25.3	32.3
^{120}Sn	32.59	9.1	10.7	15.6	19.0	19.2	24.9	30.7	25.6	31.9
^{122}Sn	4.63	8.8	11.4	15.0	20.6	19.6	24.1	33.3	25.7	30.6
^{124}Sn	5.79	8.5	12.1	14.4	22.1	20.0	23.3	35.4	25.8	29.4

currently no reliable data for the cross sections $\sigma(\gamma, 3nX)$, $\sigma(\gamma, 4nX)$, ... for tin isotopes.

Different methods are commonly used to identify neutrons produced in (γ, nX) and $(\gamma, 2nX)$ reactions. For example, in experiments on quasi-monoenergetic annihilation (QMA) photon beams, the multiplicity of produced neutrons is determined by measuring their average energy; in experiments on bremsstrahlung (BRA) photon beams, the contribution of neutrons with different multiplicities is considered using relations of the statistical theory of nuclear reactions [2].

The substantial differences between the procedures for separating the contributions to the GDR from reactions with different neutron multiplicities leads to noticeable differences in the results of different experiments. A number of special studies [3–6] have been devoted to determining the reasons for these differences, to developing methods to overcome them, and to joint evaluation of the results from different experiments for a large number of nuclei.

Experiments on $^{112, 114, 116, 117, 118, 119, 120, 122, 124}$Sn isotope photodisintegration [7–11] have yielded extensive data for the analysis and joint evaluation of the results of different experiments on determining total and partial photoneutron reaction cross sections. In this paper, we propose an approach conceptually free of the shortcomings of experimental procedures for neutron multiplicity sorting. It is based on experimental data on the total photoneutron reaction cross section $\sigma^{exp}(\gamma, xn)$ alone and uses the results from calculations describing the competition between different GDR decay channels to determine the contributions from reactions that produce one and two neutrons. Such an approach has become feasible in recent years, thanks to the obvious progress made in theoretical descriptions of GDR formation and decay channels and their competition with one another for a large number of nuclei (including several Sn isotopes) [12–14]. Using the theoretical model based on Fermi gas densities [13, 14], it is now possible to trace in detail the effects due to nucleus deformation, GDR configuration, and isospin splittings on GDR formation and decay.

EXPERIMENTAL DATA ON THE CROSS SECTIONS OF PHOTONEUTRON REACTIONS ON $^{112, 114, 116, 117, 118, 119, 120, 122, 124}$Sn ISOTOPES

Total photoneutron reaction cross sections (3) and partial reaction cross sections $\sigma^{exp}(\gamma, nX)$ and $\sigma^{exp}(\gamma, 2nX)$ on Sn isotopes were obtained in experiments using both BRA- [7–9] and QMA-quantum [10, 11] beams. The data on the experiments in which cross sections of photoneutron reactions on Sn isotopes were obtained are listed in Table 2.

In the BR experiments [7–9], the partial reaction cross sections were determined as follows. At various maximum bremsstrahlung spectrum energies E^{max}, the experimental yields $Y(E^{max})$

$$Y(E^{max}) = \alpha \int_{E_{th}}^{E^{max}} W(E^{max}, E)\sigma(E)dE, \qquad (4)$$

of the total neutron yield (3) were measured, where $\sigma(E)$ is the cross section $\sigma(\gamma, xn)$ of the reaction with threshold E_{th} at the photon energy E; $W(E^{max}, E)$ is the bremsstrahlung spectrum with upper boundary E^{max}; α is the normalization factor; and the cross section $\sigma(E)$ of the (γ, xn) reaction was determined by solving the system of integral equations (4) using the Penfold–Leiss method with a variable processing step.

To consider double contributions of the cross sections $\sigma^{exp}(\gamma, 2nX)$ to the cross section $\sigma^{exp}(\gamma, xn)$, authors introduced corrections calculated by formulas of the statistical theory [2], using the level density parameters of an individual nucleus. Using these corrections, the

Table 2. List of the data on the cross sections of photoneutron reactions on the studied Sn isotopes

Isotope	$\sigma^{exp}(\gamma, xn)$		$\sigma^{exp}(\gamma, nX)$		$\sigma^{exp}(\gamma, 2nX)$	
	BRA	QMA	BRA	QMA	BRA	QMA
^{112}Sn	[7]		[7]*		[7]**	
^{114}Sn	[8]		[8]*		[8]**	
^{116}Sn	[8]	[10, 11]	[8]*	[10, 11]	[8]**	[10, 11]
^{117}Sn	[8]	[10, 11]	[8]*	[10, 11]	[8]**	[10, 11]
^{118}Sn	[7]	[12, 13]	[7]*	[10, 11]	[7]**	[10, 11]
^{119}Sn	[8, 9]	[10]	[9]*	[10]	[9]**	[10]
^{120}Sn	[7]	[10, 11]	[7]*	[10, 11]	[7]**	
^{122}Sn	[8]		[8]*		[8]**	
^{124}Sn	[8]	[10, 11]	[8]*	[10, 11]	[8]**	[10, 11]

Notes: * Data on the cross sections $\sigma^{exp}(\gamma, nX)$ obtained according to the data in [7–9] (see below, (7)).
** Data on the cross sections $\sigma^{exp}(\gamma, 2nX)$ obtained according to the data in [7–9] (see below, (6)).

total photoneutron cross section $\sigma(\gamma, sn)$ was determined as

$$\sigma^{exp}(\gamma, sn) = \sigma^{exp}(\gamma, nX) + \sigma^{exp}(\gamma, 2nX) = \sigma^{exp}(\gamma, xn) - \sigma^{exp}(\gamma, 2nX). \quad (5)$$

We used published data [7–9] on the cross sections for reactions $\sigma^{exp}(\gamma, xn)$ and $\sigma^{exp}(\gamma, sn)$ to obtain the cross sections for reactions $\sigma^{exp}(\gamma, nX)$ and $\sigma^{exp}(\gamma, 2nX)$ (denoted by the symbols * and ** in Table 2),

$$\sigma^{exp}(\gamma, 2nX) = \sigma^{exp}(\gamma, xn) - \sigma^{exp}(\gamma, sn), \quad (6)$$

$$\sigma^{exp}(\gamma, nX) = \sigma^{exp}(\gamma, sn) - \sigma^{exp}(\gamma, 2nX) = \sigma^{exp}(\gamma, xn) - 2\sigma^{exp}(\gamma, 2nX). \quad (7)$$

In the QMA experiments (National Livermore Laboratory, United States [10], and Nuclear Research Center, Saclay, France [11]), the measurements were performed in three stages.

(i) The reaction yield $Y_{e^+}(E)$ (4) under the combined effect of positron annihilation photons and their bremsstrahlung was measured.

(ii) The reaction yield $Y_{e^-}(E)$ (4) under the effect of electron bremsstrahlung photons only was measured.

(iii) The result (after corresponding normalization and under the assumption that the positron and electron bremsstrahlung spectra were identical) was the difference between the experimental yields $Y_{e^+}(E)$ and $Y_{e^-}(E)$, which was interpreted as the desired cross section,

$$Y_{e^+}(E) - Y_{e^-}(E) = Y(E) \approx \sigma(E). \quad (8)$$

The dependence of the multiplicity of neutrons on their average energy was used in [10, 11] to separate the photoneutron reactions that produce one and two (or more) neutrons. This dependence was determined in [10] using the ring-ratio technique, in which it was assumed that the ratio of the number of counts in counters positioned at different distances from the target increases monotonically with the average neutron energy. In [11], precision calibration of liquid scintillator using a radioactive source was used to determine the average neutron energy.

SYSTEMATIC DISCREPANCIES IN EXPERIMENTAL DATA ON THE CROSS SECTIONS OF PHOTONEUTRON REACTIONS ON $^{112, 114, 116, 117, 118, 119, 120, 122, 124}$Sn ISOTOPES

Due to the substantially different procedures for separating the contributions from (γ, nX) and $(\gamma, 2nX)$ reactions, the experimental results in [7–11] exhibit certain differences [3, 5, 6, 15] that mostly appear in the energy region above the B_{2n} thresholds of reactions that produce two neutrons. Table 3 lists the results from a comparison of the partial cross sections obtained in the QMA experiments [10, 11].

The observed differences in the results from the QMA and BR experiments are shown in Fig. 1 by the example of the ^{120}Sn nucleus:

(i) The magnitudes of the cross sections $\sigma^{exp}(\gamma, nX)$ [11] are larger than those of the cross sections obtained in [10] and [7–9], which are close to one another.

(ii) The magnitudes of the $\sigma^{exp}(\gamma, 2nX)$ cross sections are smaller than those of the cross sections obtained in [10] and [7–9]; in those cases, the cross sections of [7–9] have the largest values.

The data given in Table 3 confirm in general the problems considered in [3–6] and associated with the insufficient reliability of the methods for sorting partial photoneutron reaction multiplicity in QMA experiments. One disadvantage of the BR experiments

Table 3. Data [6] on the ratios of the integrated cross sections of the (γ, nX) and (γ, 2nX) reactions, obtained at Saclay [11] and Livermore [10] ($E_{\text{int min}}$ and $E_{\text{int max}}$ are the lower and upper integration limits)

Nucleus	$E_{\text{int min}}$, MeV	$E_{\text{int max}}$, MeV	$R(\text{n}) = \sigma^{\text{S}}_{\text{int}}(\gamma, \text{n}X)/\sigma^{\text{L}}_{\text{int}}(\gamma, \text{n}X)$, rel. units	$R(2\text{n}) = \sigma^{\text{S}}_{\text{int}}(\gamma, 2\text{n}X)/\sigma^{\text{L}}_{\text{int}}(\gamma, 2\text{n}X)$, rel. units
^{116}Sn	17.1	22.1	1.10	0.92
^{117}Sn	16.7	21.1	1.02	0.93
^{118}Sn	16.3	21.6	1.07	0.86
^{120}Sn	15.6	22.4	1.00	0.86
^{124}Sn	14.6	21.6	0.93	0.94

is their use of statistical theory relations to determine the contribution from the partial cross section $\sigma^{\text{exp}}(\gamma, \text{n}X)$ to the total cross section $\sigma^{\text{exp}}(\gamma, x\text{n})$, whereas (as is known [16, 17]) direct processes make a rather noticeable contribution (as high as ~20%) to the photodisintegration of nuclei.

At the same time, the data in Table 3 (see also Fig. 1) show that the discussed differences in the cross sections of reactions with different multiplicities are relatively small for the Sn isotopes under study. This allows us to compare the cross sections $\sigma^{\text{eval}}(\gamma, \text{n}X)$ and $\sigma^{\text{eval}}(\gamma, 2\text{n}X)$ evaluated within the proposed method with the experimental data.

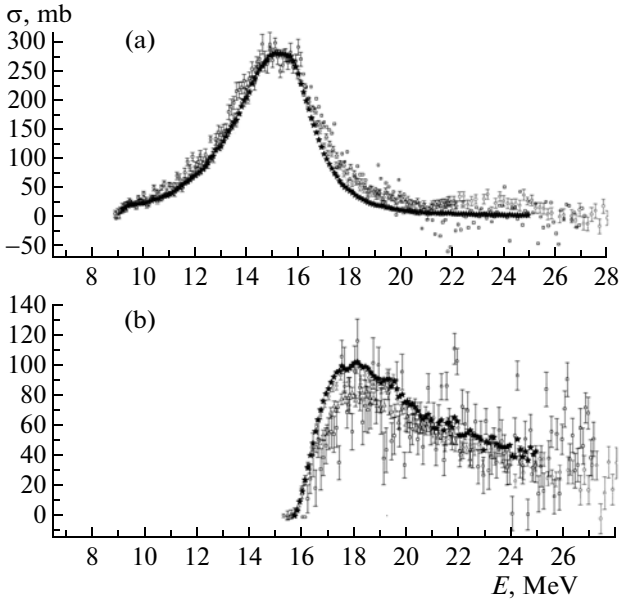

Fig. 1. Comparison of the experimental data in [7] (relations (8) and (9), squares), [10] (circles), [11] (triangles) and the evaluated ($\sigma^{\text{eval-joint}}$, closed stars, see below, (14) and (15) partial photoneutron reactions cross sections for the ^{120}Sn isotope ($B_{2\text{n}} = 15.6$ MeV): (a) ^{120}Sn(γ, nX) and (b) ^{120}Sn(γ, 2nX).

A NEW APPROACH TO ANALYZING DATA ON PARTIAL PHOTONEUTRON REACTION CROSS SECTIONS

In view of the above, we propose a new approach, largely free of the shortcomings of the experimental sorting of photoneutrons according to multiplicity, to jointly evaluate the partial cross sections of photoneutron reactions on Sn isotopes. It uses only the data on the cross section $\sigma^{\text{exp}}(\gamma, x\text{n})$ as its initial experimental information, and the relations between the cross sections $\sigma^{\text{theor}}(\gamma, x\text{n})$, $\sigma^{\text{theor}}(\gamma, \text{n}X)$, and $\sigma^{\text{theor}}(\gamma, 2\text{n}X)$, calculated within the theoretical model [13, 14, 18] to describe the competition of GDR decay channels, to separate the contributions from the (γ, nX) and (γ, 2nX) partial reactions to this cross section. The main relations of the pre-equilibrium model of photonucleon reactions, based on Fermi gas densities, are given in [15].

As an example (^{124}Sn), Fig. 2 shows the reaction cross sections calculated [13, 14] up to energies of ~100 MeV for pure neutron (γ, 0pkn) GDR decay channels and the strongest of the other decay channels that produce one (γ, 1pkn) or two (γ, 2pkn) protons. The competition between different GDR decay channels is easily seen.

Within the proposed method for separating the competing (γ, nX), (γ, 2nX), ... reactions, the cross sections of reactions producing one or two neutrons were evaluated as follows.

(i) The theoretically calculated [13, 14] cross sections $\sigma^{\text{theor}}(\gamma, \text{n}X)$, $\sigma^{\text{theor}}(\gamma, 2\text{n}X)$..., ... were combined into the total photoneutron reaction cross section:

$$\sigma^{\text{theor}}_{(\gamma, x\text{n})}(E) = \sigma^{\text{theor}}_{(\gamma, \text{n}X)}(E) + 2\sigma^{\text{theor}}_{(\gamma, 2\text{n}X)}(E) + \dots . \quad (9)$$

(ii) For each photon energy E, a multiplicity transition function $F(E)$ was constructed that described the contribution from the cross section of the reaction producing two neutrons to the total reaction cross section (Fig. 3):

$$F(E) = \sigma^{\text{theor}}_{(\gamma, 2\text{n}X)}(E)/\sigma^{\text{theor}}_{(\gamma, x\text{n})}(E) = \sigma^{\text{theor}}_{(\gamma, 2\text{n}X)}(E)/[\sigma^{\text{theor}}_{(\gamma, \text{n}X)}(E) + 2\sigma^{\text{theor}}_{(\gamma, 2\text{n}X)}(E) + \dots]. \quad (10)$$

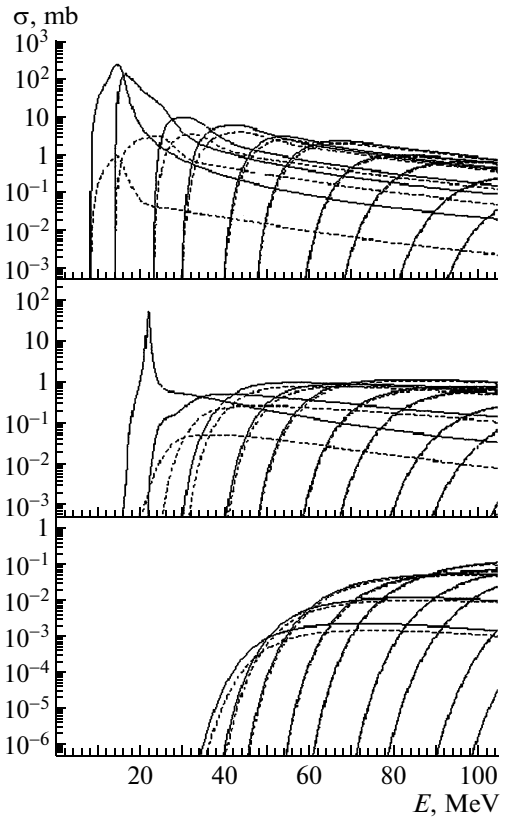

Fig. 2. Calculated [13, 14] reaction cross sections (from the top down: (γ, 0p*k*n), (γ, 1p*k*n), and (γ, 2p*k*n)) for the ^{124}Sn: the total cross section (solid curves) and the contribution of the quasi-deuteron component (dashed curves).

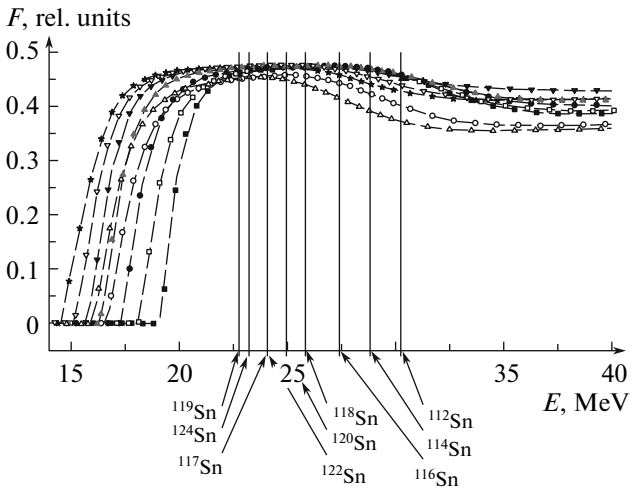

Fig. 3. Energy dependences of the transition functions $F(E)$ describing the contribution from the partial cross section $\sigma^{theor}(\gamma, 2nX)$ to the total photoneutron reaction cross section $\sigma^{theor}(\gamma, xn)$ for the studied Sn isotopes (arrows at the bottom indicate the (γ, 3n) reaction threshold B_{3n}): ^{112}Sn (closed squares), ^{114}Sn (open squares), ^{116}Sn (closed circles), ^{117}Sn (open circles), ^{118}Sn (closed triangles), ^{119}Sn (open triangles), ^{120}Sn (inverted closed triangles), ^{122}Sn (inverted open triangles), and ^{124}Sn (stars).

(iii) Using the $F(E)$ and experimental data on the total photoneutron reaction cross section $\sigma^{exp}(\gamma, xn)$ (3), the cross sections evaluated by the experimental data were obtained for each experiment [7, 8, 10, 11]:

$$\sigma^{eval}_{exp(\gamma,2nX)}(E) = F(E)\sigma^{exp}_{(\gamma,xn)}(E); \quad (11)$$

$$\sigma^{eval}_{exp(\gamma,nX)}(E) = \sigma^{exp}_{(\gamma,xn)}(E) - 2\sigma^{eval}_{exp(\gamma,2nX)}(E) = \sigma^{exp}_{(\gamma,xn)}(E) - 2F(E)\sigma^{exp}_{(\gamma,xn)}(E) = (1 - 2F(E))\sigma^{exp}_{(\gamma,xn)}(E). \quad (12)$$

Note that the model in [13, 14] considers the basic mechanisms controlling the competition of different decay channels of excited nucleus states in the GDR region, and the properties of function F following from definition (10) make this function a very convenient tool for analyzing the reliability of separating the contributions from processes with the emission of one or two neutrons.

Figure 3 shows the energy dependences of the transition functions $F(E)$, as calculated for all of the studied Sn isotopes. They have the following characteristic features:

(i) According to definition (10), $F(E)$ is characterized by a threshold behavior, since its numerator contains the threshold quantity $\sigma(\gamma, 2nX)$: $F(E) = 0$ in the energy region below the $\sigma(\gamma, 2n)$ reaction threshold B_{2n}; immediately above the threshold B_{2n} $F(E)$ increases sharply and reaches a maximum at 2–3 MeV.

(ii) According to definition (10), the function $F(E)$ cannot be larger than 0.5 at any photon energy; for each of the studied Sn isotopes, the function $F(E)$ reaches a maximum in a flat sector ~4–6 MeV wide, in which $F(E) \approx$ const = 0.46–0.48. It should be noted that the appearance of values exceeding 0.5 in the corresponding ratio $\sigma^{exp}_{(\gamma,2nX)}(E)/\sigma^{exp}_{(\gamma,xn)}(E)$ of the experimental cross sections suggests the presence of significant errors in determining the partial reaction cross sections, especially when nonphysical negative values appear in the partial cross section $\sigma(\gamma, nX)$.

(iii) At energies behind the GDR maximum, the function $F(E)$ decreases rather rapidly to ~0.40–0.45; a comparison of these data with the data of Table 1 allows us to conclude that the decrease in $F(E)$ in the energy region behind the GDR maximum is due to a new GDR decay channel with three-nucleon emission opening in this energy region (i.e., the appearance of the term $3\sigma^{theor}_{(\gamma,3nX)}(E)$) in relation (10)).

(iv) The values of E at which the values of $F(E)$ appreciably decrease vary smoothly from ~23 to ~30 MeV when going from the heaviest isotope (^{124}Sn) to the lightest (^{112}Sn).

The relatively weak dependence of $F(E)$ on the γ-quantum energy as the latter continues to rise testifies to the relatively weak energy dependence of the

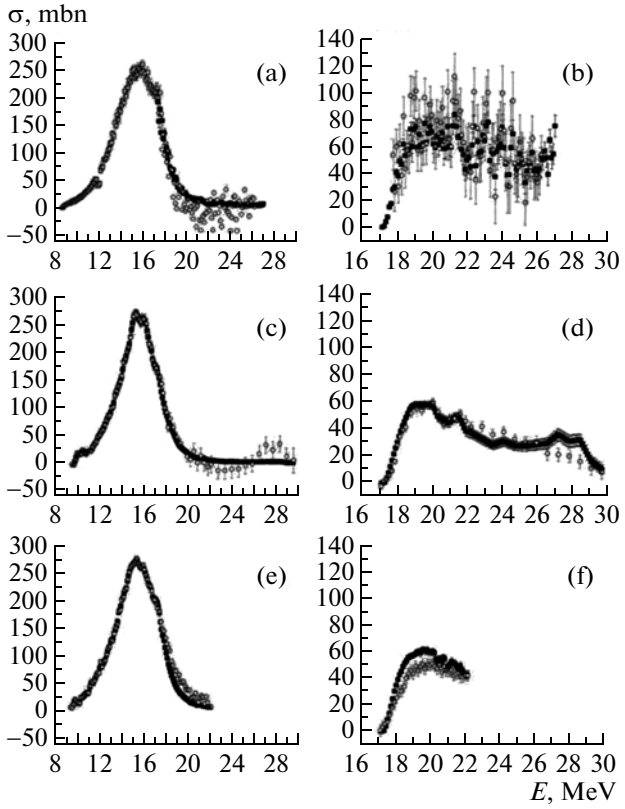

Fig. 4. Comparison of the experimental (open circles) and evaluated (relations (11) and (12), closed squares) data on the partial reaction cross sections (a, c, e) $\sigma^{eval}_{exp}(\gamma, nX)$ and (b, d, f) $\sigma^{eval}_{exp}(\gamma, 2nX)$ of reactions on the ^{16}Sn isotope according to the data of (a, b) [8], (c, d) [10], and (e, f) [11].

γ-quantum absorption cross section in this region, i.e., behind the GDR maximum ($E \geq 35$ MeV).

It should also be noted that in the above situation, the contributions from processes with the emission of three neutrons have no any appreciable effect on the proposed approach for separating the $\sigma(\gamma, nX)$ and $\sigma(\gamma, 2nX)$ reaction cross sections for Sn isotopes with the cross sections $\sigma(\gamma, 3nX)$. When the $(\gamma,3n)$ reaction thresholds B_{3n} are especially low, however, and their magnitudes are appreciable in comparison with the cross sections $\sigma(\gamma, 2nX)$, the proposed approach should be modified (generalized) by introducing the additional multiplicity transition functions

$$F_i(E) = \sigma^{theor}_{(\gamma,inX)}(E)/\sigma^{theor}_{(\gamma,xn)}(E), \quad (13)$$

each of which describes the contribution from the corresponding i-th partial reaction to the $\sigma(\gamma, xn)$ reaction cross section.

For all of the studied $^{112, 114, 116–120, 122, 124}$Sn isotopes, the data on both partial reaction cross sections, $\sigma^{eval}_{exp(\gamma,2nX)}$ [7, 8, 10, 11] and $\sigma^{eval}_{exp(\gamma,nX)}$ [7, 8, 10, 11], evaluated using experimental data on the cross sections $\sigma^{exp}_{(\gamma,xn)}$, were compared with the results of corresponding experiments (Fig. 4 shows the example for the ^{116}Sn nucleus). This allowed us to conclude that good agreement is generally observed for all of the studied Sn isotopes, in terms of the energy position, magnitude, and shape of the partial cross sections $\sigma(\gamma, nX)$ and $\sigma(\gamma, 2nX)$ obtained by the four following methods:

(i) separating the contributions from partial reactions to the total photoneutron reaction cross section, using the relations of the statistical model of photonuclear reactions in BRA experiments;

(ii) direct photoneutron multiplicity sorting in the QMA experiment in [10];

(iii) direct photoneutron multiplicity sorting in the QMA experiment in [11];

(iv) determining the contributions from the partial reaction cross sections to the experimental total photoneutron cross section $\sigma(\gamma, xn)$, using our method.

In the next stage, the partial reaction cross sections evaluated using the data of the individual experiments were used in the joint evaluation procedure

$$\sigma^{eval\text{-}joint}(E) = \frac{\sum_i (\Delta\sigma(E)_i)^{-2}\sigma(E)_i}{\sum_i (\Delta\sigma(E)_i)^{-2}}, \quad (14)$$

where $i = 1, 2, 3$ numerates one of the cross sections, $\sigma_i(\sigma^{eval}_{exp}(\gamma,nX)$ or $\sigma^{eval}_{exp}(\gamma,2nX))$, evaluated with the uncertainty $\Delta\sigma_i$ by the method described above. The uncertainty of the evaluated cross section was calculated using the relation

$$\Delta\sigma^{eval\text{-}joint} = \frac{1}{\sum_i (\Delta\sigma(E)_i)^{-2}}\sqrt{\sum_i (\Delta\sigma(E)_i)^{-2}}. \quad (15)$$

A comparison of the partial cross sections $\sigma^{eval\text{-}joint}_{(\gamma,nX)}(E)$ and $\sigma^{eval\text{-}joint}_{(\gamma,2nX)}(E)$, evaluated using the results from several experiments with the data obtained in individual experiments (an example is shown in Fig. 1), suggests that the proposed model adequately describes the experimental data for the partial cross sections of both photonuclear reactions corresponding to two main GDR decay channels.

Table 4 lists the data on the integrated cross sections of partial reactions, as calculated by the cross sections evaluated for two energy regions, i.e., from the $(\gamma,2n)$ reaction threshold B_n to the $(\gamma,2n)$ reaction threshold B_{2n} and from B_{2n} to the $(\gamma,3n)$ reaction threshold B_{3n}. These data reveal complex relations between processes with the emission of several neutrons in the GDR maximum region. For example, even for the lightest ^{112}Sn isotope, due to the relatively low $(\gamma,2n)$ reaction threshold $B_{2n} = 19.0$ MeV, a major part of the (γ, nX) cross section in the GDR maximum region appears in the energy region in which the emis-

Table 4. Comparison of the integral characteristics σ_{int} of the evaluated cross sections $\sigma^{eval\text{-}joint}_{(\gamma, nX)}(E)$ and $\sigma^{eval\text{-}joint}_{(\gamma, 2nX)}(E)$ determined for different γ-quantum energy ranges

Nucleus	B_n, MeV	$\sigma_{int}(B_{2n} - B_n)$, MeV mb	B_{2n}, MeV	$\sigma_{int}(B_{3n} - B_{2n})$, MeV mb		B_{3n}, MeV
		(γ, nX)		(γ, nX)	(γ, 2nX)	
^{112}Sn	10.8	1370	19.0	163*	359*	30.2
^{114}Sn	10.3	1150	18.0	249*	442*	28.8
^{116}Sn	9.6	1030	17.1	284	408	27.4
^{117}Sn	6.9	928	16.5	390	402	24.1
^{118}Sn	9.3	851	16.3	339	510	25.8
^{119}Sn	6.5	775	15.8	456	409	22.7
^{120}Sn	9.1	799	15.6	423	607	24.9
^{122}Sn	8.8	591	15.0	456	493	24.1
^{124}Sn	8.5	503	14.4	535	635	23.3

* Measurements were made up to the energy $E = 27$ MeV (below the (γ, 3n) reaction threshold B_{3n}).

Table 5. Comparison of the main GDR parameters in the $\sigma^{eval\text{-}joint}(\gamma, sn) \approx \sigma(\gamma, abs)$ evaluated cross sections with the experimental data (E_m is the maximum position, σ_m is the cross section at the maximum, Γ is the maximum width)

Nucleus	E_m, MeV				σ_m, mb				Γ, MeV			
	[7, 8]	[10]	[11]	Eval.	[7, 8]	[10]	[11]	Eval.	[7, 8]	[10]	[11]	Eval.
^{112}Sn	15.8	–	–	15.8	268	–	–	270	5.9	–	–	5.3
^{114}Sn	15.7	–	–	15.8	265	–	–	265	7.0*	–	–	5.5
^{116}Sn	15.6	15.7	15.6	15.6	260	266	270	270	6.0*	4.2	5.2	4.7
^{117}Sn	15.4	15.7	15.7	15.6	260	254	255	260	5.5*	5.0	5.3	4.8
^{118}Sn	15.5	15.6	15.4	15.5	272	255	278	265	5.8	4.8	5.0	4.5
^{119}Sn	15.4	15.5	–	15.6	270	253	–	255	6.0*	4.9	–	5.0
^{120}Sn	15.3	15.4	15.4	15.4	297	280	284	285	5.7	4.8	5.3	4.5
^{122}Sn	15.6	–	–	15.2	270	–	–	270	5.0*	–	–	4.3
^{124}Sn	15.5	15.2	15.3	15.1	270	283	275	280	5.5*	5.2	5.0	4.3

* Measurements absent in the original publications are taken from [19].

sion of two neutrons is possible. In going to the ^{124}Sn heavy isotope, the thresholds B_n, B_{2n}, and B_{3n} of reactions with emission of one, two, and three neutrons decrease by 2.3, 4.6, and 6.9 MeV, respectively. As the numbers of neutrons in the nucleus increases, the energy region in which GDR decays with the emission of one neutron can be clearly identified narrows continuously, while the region of the competition between such processes and those with the emission of two neutrons broadens. For example, beginning with the ^{117}Sn isotope, the total reaction cross sections $\sigma_{(\gamma,nX)}(E)$ and $\sigma_{(\gamma,2nX)}(E)$ in the energy range $B_{3n} - B_{2n}$ appear almost comparable. In this case, beginning with the energy of ~23–24 MeV, the (γ, 3n) reaction is added to competing reactions.

In Table 5, the main parameters of the evaluated cross sections $\sigma^{eval\text{-}joint}(\gamma, sn) = \sigma^{eval\text{-}joint}(\gamma, nX) + \sigma^{eval\text{-}joint}(\gamma, 2nX)$, calculated using Lorentzian curves, are compared to the corresponding parameters of the experimental reaction cross sections [7, 8, 10, 11].

Table 6 compares the integrated cross sections calculated using the experimental and evaluated data. The highest energies to which the integrated reaction cross sections were calculated are indicated.

We can see that the evaluated cross sections that satisfactorily describe the relations between the cross sections $\sigma^{eval\text{-}joint}(\gamma, nX)$ and $\sigma^{eval\text{-}joint}(\gamma, 2nX)$ are in agreement with the experimental data on the total photoneutron cross sections. The above considerations allow certain conclusions to be drawn as to the behavior of GDR parameters as the isotope mass number A varies:

Table 6. Comparison of the data on the integrated cross sections σ_{int} for the evaluated total photoneutron cross sections $\sigma^{eval\text{-}joint}(\gamma, sn) \approx \sigma(\gamma, abs)$ with the experimental data

Nucleus	B_{3n}, MeV	Integrated cross sections σ_{int} of the $\sigma(\gamma, sn)$ photoneutron reaction					
		[7, 8], <27 MeV	[10], <30 MeV	[11], <30 MeV	Evaluation, ($<B_{3n}$)	Evaluation, total	Dipole sum rule, 60 *NZ/A*
	MeV	MeV mb					
^{112}Sn	30.2	1900*			1893	1893	1661
^{114}Sn	28.8	1860*			1841	1841	1684
^{116}Sn	27.4	1850	1667	1860	1719	1778	1707
^{117}Sn	24.1	1860	1939	1570**	1720	1956	1718
^{118}Sn	25.8	1920	1898	1690**	1700	1840	1729
^{119}Sn	22.8	1860	2078		1640	2042	1739
^{120}Sn	24.9	2070	2092	2140	1855	2013	1750
^{122}Sn	24.1	2030			1685	1887	1770
^{124}Sn	23.3	1930	2077	1620**	1674	1925	1790

Notes: * Measurements were performed up to the energy below the $(\gamma, 3n)$ reaction threshold B_{3n}.
** Data up to the energy $E = 23$ MeV.

(i) According to the known laws, the GDR maximum position E_m shifts to lower γ-quantum energies when moving to a heavier isotope.

(ii) When moving from the ^{112}Sn isotope to ^{124}Sn, the GDR narrows, since the number of neutrons in the nucleus approaches the magic number $N = 82$.

(iii) The σ_m cross section at the GDR amplitude remains approximately constant.

The above data suggest that the GDR integrated cross section (the cross section $\sigma^{eval\text{-}joint}(\gamma, sn) \approx \sigma(\gamma, abs)$ evaluated within the approach described above) remains almost unchanged when moving from the ^{112}Sn light isotope to the ^{124}Sn heavy isotope. At the same time, the total cross section $\sigma^{eval\text{-}joint}(\gamma, nX)$ decreases, while $\sigma^{eval\text{-}joint}(\gamma, 2nX)$ increases (see also Table 4), due to a diminution of the difference $E_m - B_{2n}$ between the GDR maximum's position and the (γ,2n) reaction threshold. The integrated reaction cross section $\sigma^{eval\text{-}joint}(\gamma, sn) \approx \sigma(\gamma, abs)$ remains almost unchanged, while, according to estimations by the dipole sum rule, the GDR should increase.

ACKNOWLEDGMENTS

This study was supported by the Russian Foundation for Basic Research, project no. 09-02-00368; Grant for the Support for Leading Scientific Schools no. 02.120.21.485-NSh; the Federal Agency on Science and Innovations, contract no. 02.740.11.0242 (Initiative 1.1, Scientific Research by Teams of Scientific and Educational Centers); and State Contract no. 2009-1.1-125-055.

REFERENCES

1. *Kal'kulyator i graficheskaya sistema dlya parametrov atomnykh yader i kharakteristik yadernykh reakcij i radioaktivnykh raspadov, CDFE NIIYaF MGU* (Calculator and Graph Engine for Atomic Nuclei Parameters and Nuclear Reactions and Radioactive Decays Features, MSU SINP CDFE). Available from: http://sdfe.sinp.msu.ru/services/calc_thr/calc_thr_ru.html
2. Bohr, A. and Mottelson, B.R., *Nuclear Structure,* New York: Benjamin, 1969, vol. 2.
3. Wolynec, E. and Martins, M.N., *Revista Brasileira Fisica*, 1987, vol. 17, p. 56.
4. Berman, B.L., Pywell, R.E., Dietrich, S.S., et al., *Phys. Rev. C*, 1987, vol. 36, p. 1286.
5. Varlamov, V.V. and Ishkhanov, B.S., *INDC(CCP)-433, IAEA NDS*, Vienna, 2002.
6. Varlamov, V.V., Peskov, N.N., Rudenko, D.S., et al., *Vopr. Atomn. Nauki Tekhn. Yad. Konst.,* 2003, vol. 1–2, p. 48.
7. Sorokin, Yu.I. and Yur'ev, B.A., *Yad. Fiz.,* 1974, vol. 20, p. 233.
8. Sorokin, Yu.I. and Yur'ev, B.A., *Izv. AN. SSSR, Ser. Fiz.*, 1975, vol. 39, no. 1, p. 114.
9. Sorokin, Yu.I., Khrushchev, V.A., and Yur'ev, B.A., *Izv. AN. SSSR, Ser. Fiz.*, 1972, vol. 36, no. 1, p. 180.
10. Fultz, S.C., Berman, B.L., Caldwell, J.T., et al., *Phys. Rev.*, 1969, vol. 186, p. 1255.
11. Lepretre, A., Beil, H., Bergere, R., et al., *Nucl. Phys. A,* 1974, vol. 219, p. 39.
12. Chadwick, M.B., Oblozinsky, P., Hodgson, P.E., et al., *Phys. Rev. C*, 1991, vol. 44, p. 814.
13. Ishkhanov, B.S. and Orlin, V.N., *Fiz. Elem. Chastits At. Yadra*, 2007, vol. 38, p. 460 [*Phys. Part. Nucl.* (Engl. Transl.), 2007, vol. 38, no. 2, p. 232].

14. Ishkhanov, B.S. and Orlin, V.N., *Yad. Fiz.*, 2008, vol. 71, p. 517 [*Phys. At. Nucl.* (Engl. Transl.), 2008, vol. 71, no. 3, p. 397].
15. Varlamov, V.V., Ishkhanov, B.S., Orlin, V.N., et al., *Preprint of NIIYaF MGU–2009–3/847*, Moscow, 2009.
16. Berman, B.L. and Fultz, S.C., *Rev. Mod. Phys.,* 1975, vol. 47, p. 713.
17. Varlamov, V.V., Gudenko, Yu.Yu., Komarov, S.Yu., et al., *Sb. tez. dokl.: 56-ya Mezhdunar. konf. po problemam yadernoi spektroskopii i strukture atomnogo yadra "Yadro-2006"* (Proc. 56th Int. Conf. on on Nuclear Spectroscopy and Atomic Nuclear Structure "Nuclear–2006"), Sarov: RFYaTs VNIIEF, Sept. 4–8 2006, p. 37.
18. Laget, J.M, in *Lecture Notes Physics*, Arenhovel, H. and Saruis, A.M., Eds., Berlin: Springer–Verlag, 1981, vol. 137, p. 148.
19. Varlamov, A.V., Varlamov, V.V., Rudenko, D.S., et al., *INDC(NDS)–394, IAEA NDS*, Vienna, 1999.